

Superconductivity and the new Fe Based Superconductors

The Imperial College group has a long-established programme on superconductivity, going back to before the discovery of the high temperature superconductors (HTS) in 1986, evolving from vortex physics, superconducting critical current density and distribution of critical current in wires and tapes for power transmission, to more microscopic aspects and other interests such as dc metamaterials (so called invisibility cloaking at dc).¹ Our wide research portfolio has stimulated the development of a suite of novel specialised experimental techniques that are applicable to a range of material classes including superconductors.

In 2001 superconductivity in MgB₂ was discovered and the group were well placed to respond immediately to the discovery of these materials² and again when the families of Fe-based (or pnictide) superconductors were discovered in early 2008 we were able to make some important initial findings.^{3,4,5} We have good links to key international collaborators in the USA, China, Taiwan and Europe as well as with many groups within the UK.

Brief Summary of Fe Based Superconductors

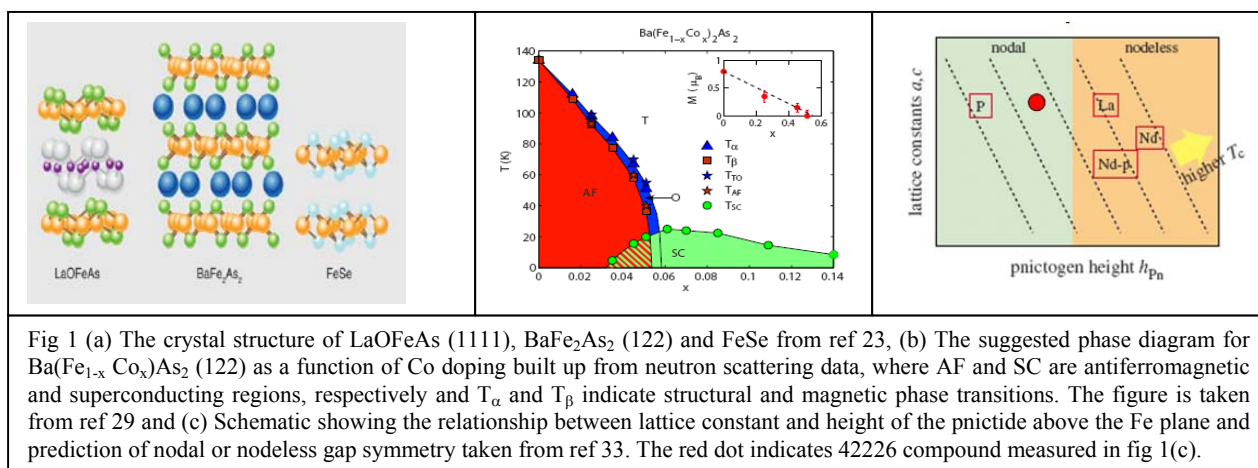


Fig 1 (a) The crystal structure of LaOFeAs (1111), BaFe₂As₂ (122) and FeSe from ref 23, (b) The suggested phase diagram for Ba(Fe_{1-x}Co_x)As₂ (122) as a function of Co doping built up from neutron scattering data, where AF and SC are antiferromagnetic and superconducting regions, respectively and T_α and T_β indicate structural and magnetic phase transitions. The figure is taken from ref 29 and (c) Schematic showing the relationship between lattice constant and height of the pnictide above the Fe plane and prediction of nodal or nodeless gap symmetry taken from ref 33. The red dot indicates 42226 compound measured in fig 1(c).

The Fe based superconductors are layered materials, see figure 1(a) where the Fe atoms are arranged on a simple square lattice⁶ and they are either pnictides (1111 and 122 being the main families studied to date) or chalcogenides (11). In the latter, superconductivity has been discovered in FeSe⁷ (T_c = 8K, up to 17K with doping and over 36K under pressure⁸). The 1111 LaNiPO, LaFePO analogues have T_c ~ few K, low enough to be accounted for by electron-phonon coupling. However, the symmetry of the order parameter in LaFePO appears to be nodal⁹, pointing to complexity in the pairing mechanism even in these lower T_c systems. There are strong electron – electron correlations, and there is clear evidence for the formation of a spin density wave (SDW) gap in the undoped pnictide compounds¹⁰ associated with a structural change in crystal symmetry. All the materials are low carrier density semi-metals, and in the doped pnictide case, on the verge of itinerant magnetism.¹¹

Interestingly the chalcogenides (FeSe) appear to have no static magnetic ordering unlike the FeAs based systems. For the pnictides there is increasing evidence of coexistence of superconductivity and magnetism on a local scale from muon and neutron studies^{12,13}, as shown in figure 1(b) for Ba(Fe_{1-x}Co_x)As₂ (122) as a function of Co doping¹⁴, but the lengthscales associated with coexistence are unclear. Recent studies in CeFeAsO_{1-x}F_x as a function of F content have shown that the doping does not change the Fe-As distance, but rather tunes (reduces) the angle between Fe-As-Fe bonds, and it is

this angle that controls the electron band width¹⁵ and so changes T_c . The main role of F doping is dual: transferring electrons to the Fe-As block and thereby affecting the electron band width; and suppression of the tetragonal to orthorhombic structural transition.^{16,17} Although the angle between Fe-As-Fe bonds is important, it has recently been shown that it is the pnictide height above the Fe layer that is the key parameter controlling the symmetry of the bands that cross the Fermi surface, and also the resulting symmetry of the spin fluctuations.¹⁸ The prediction shown in fig 1(c) is that the symmetry of the superconducting order parameter should change from nodal to nodeless as the pnictide height above the Fe layer increases. Systems that are at or close to the crossover are the most interesting to study; the 42226 compound on this schematic (large red circle) is a high-priority candidate. Although there is no consensus theoretically concerning the symmetry of the order parameter, and perhaps given this recent prediction this shouldn't be expected, the extended s wave model is finding considerable favour.^{19,20}

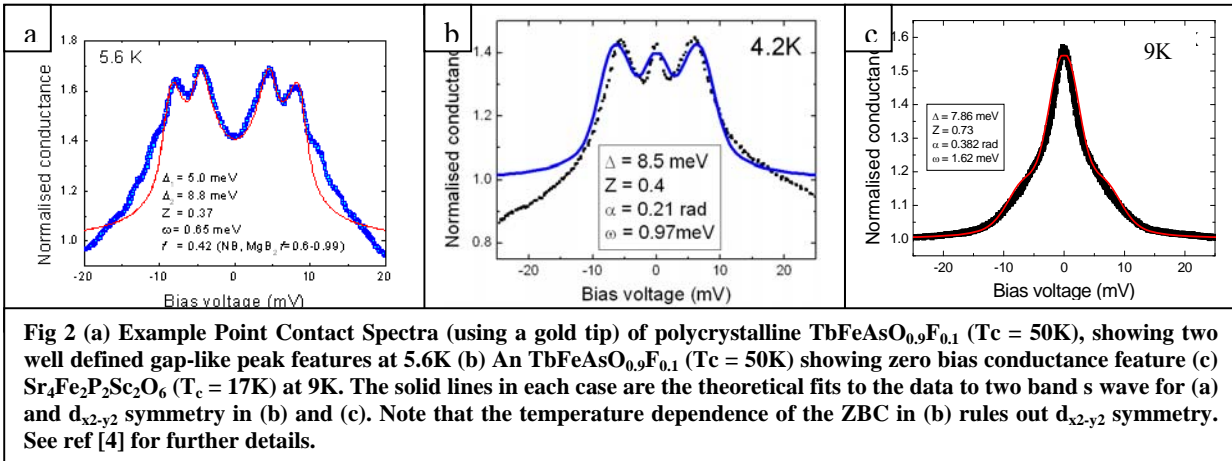
Interestingly, one aspect of this extended s wave model is the role of non-magnetic impurities: In a multi-gap superconductor non-magnetic defects that promote interband scattering can be deleterious to the superconductivity, just as magnetic impurities destroy superconductivity in single band s wave superconductors; this prediction has yet to be verified. So far nothing at all is known systematically about the defects in these materials or their fundamental role in supporting or destroying the superconductivity (preliminary studies have been undertaken of the effect of point and line defects on the critical current density and critical fields in both 1111 and 122 materials^{21,22}).

The mechanism for superconductivity in pnictides seems to be accepted as related to magnetic spin fluctuations, and although proximity to magnetism is similar in pnictides and HTS, the shape of the Fermi surfaces and the nature of the magnetism in the two systems (in cuprates the parent compound is an AFM insulator and in the pnictides it is an AFM semimetal) requires that the precise pairing mechanism and associated order parameter symmetries differ.

Research at Imperial College on Fe Based Superconductors

1 Superconducting Energy Gap and Andreev Point Contact Spectroscopy

Point contact spectroscopy (PCS) was developed to chart the evolution of the superconducting energy gap (Δ) in magnetic field.²³ In multi-parameter fitting it is essential to use rigorous methods to extract parameters uniquely,²⁴ and we have developed a robust two-channel model to interpret PCS data in applied magnetic field, showing that for type II superconductors, an additional form of broadening occurs in finite magnetic field associated with the presence of the mixed state^{25,26}. An extension of this model was used to extract the electron diffusivity ratio, η , between the two bands in epitaxial thin films of MgB₂ superconductors.^{27,28} We have explored the relationship between the η extracted from direct $H_{c2}(T)$ measurements and that obtained by PCAR techniques and find good agreement between the two approaches.²⁹ In the oxypnictides we have so far made measurements on polycrystalline oxygen-deficient NdFeAsO_{0.85}, $T_c = 45.5\text{K}$ [3] and TbFeAsO_{0.9}F_{0.1} ($T_c = 50\text{K}$) [4] and Sr₄Fe₂P₂Sc₂O₆ ($T_c = 17\text{K}$) [30]. Representative data on these samples are shown in figure 2.



2 Magnetic Characterisation and Imaging

Measurement of the key parameter for applications, the critical current density J_c , is often complicated by poor connectivity at grain boundaries. We have developed the simple “length-scale” analysis for examining this issue³¹ that is a prerequisite for meaningful studies of flux pinning and so for the enhancement of J_c . For MgB_2 studies we have improved the sensitivity of the approach by adding an AC modulation to the background field (“AC length-scale analysis”). In addition to conventional (magnetic or transport) measurement of those parameters, we can monitor J_c locally – on a scale of microns - with our scanning Hall probe microscope as shown in figure 3(a).³² Although usually used for imaging (up to much higher fields than attainable with magnetooptics), it is equally well adapted to high-field magnetic studies of very small samples, and it can also be used to extract H_{c2} .³³ Given the background ferromagnetic signal present in many samples most useful imaging has to be done at fields sufficient to saturate the FM and therefore only Hall probe and not magnetooptic imaging is practical here.

In addition to conventional (magnetic or transport) measurement, we can use our scanning Hall probe microscope (up to much higher fields than attainable with magnetooptics), to measure local superconducting parameters (T_c , H_{c2} , etc.)³⁴ so as to be confident of sample homogeneity. Given the background ferromagnetic signal present in some samples, useful imaging has to be done at fields sufficient to saturate the FM and therefore only Hall probe and not magnetooptic imaging is practical here.

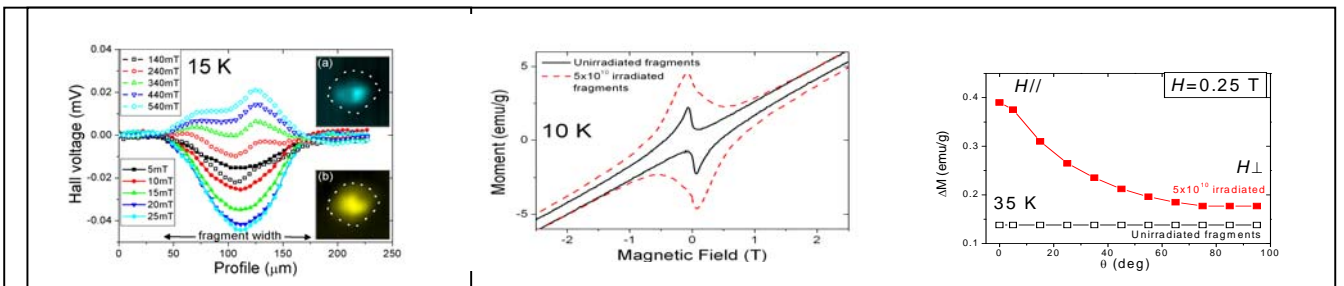


Fig 3 (a) Shows crosssections taken across Hall probe images such as those shown in the inset. These Bean-like profiles show that the fragment carries a fully connected supercurrent. In this fragment we detected both the superconducting phase (yellow) and an extrinsic paramagnetic component (blue) (b) We have begun to study the effect of defects on vortex behaviour and here we show the influence of high energy Ta ion damage (c) Shows the angular dependence of the pinning enhancement from irradiation where $\theta = 0$ is along the columnar defects. At lower temperature the pinning enhancement becomes more isotropic. All data is taken on 1111 $\text{NdFeAsO}_{0.85}$.

Measurement of the key parameter for applications, the critical current density J_c , is often complicated by poor connectivity at grain boundaries. We have developed the simple “length-scale” analysis for examining this issue³⁵ that is a prerequisite for meaningful studies of flux pinning and so for the enhancement of J_c . For MgB₂ studies we have improved the sensitivity of the approach by adding an AC modulation to the background field (“AC length-scale analysis”). In addition to conventional (magnetic or transport) measurement of those parameters, we can monitor J_c locally – on a scale of microns - with our scanning Hall probe microscope as shown in figure 2(a).³⁶ Although usually used for imaging (up to much higher fields than attainable with magneto-optics), it is equally well adapted to high-field magnetic studies of very small samples, and it can also be used to extract H_{c2} .³⁷ Given the background ferromagnetic signal present in many samples most useful imaging has to be done at fields sufficient to saturate the FM and therefore only Hall probe and not magneto-optic imaging is practical here. We have begun to explore the influence of columnar defects as shown in fig 3(b) and (c)³⁸.

See figure 4 for an example of Hall probe imaging of single crystals from Oak Ridge National Laboratory.

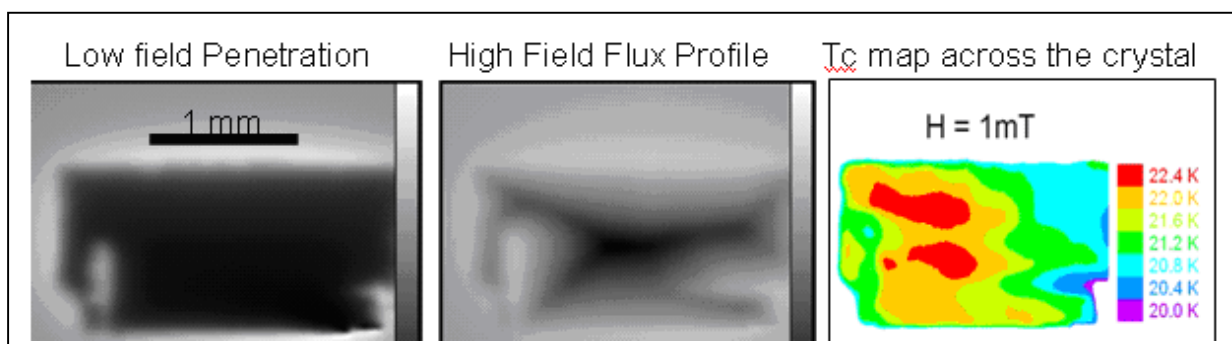


Figure 4 Characterisation of a 0.8mm x 1.2mm (approximately) 122 Ba(Fe_{1.8},Co_{0.2})As₂ single crystal using the scanning Hall probe. (a) The crystal was zero field cooled and imaged after a 60mT field was applied. The dark region across the crystal shows where the flux is excluded. The crystal supports a screening current around the edge i.e. it is fully connected. (b) Imaging at high field shows classic Bean profile (c) Here the crystal was zero field cooled at temperatures approaching T_c , 1mT applied and then the image was captured. The colour plot is an amalgamation of the imaged superconducting regions at the temperatures indicated by the colour scale.. Crystal supplied by Oak Ridge National Labs

3. Other Areas of Expertise Pertinent to Oxypnictides

Raman Spectroscopy: This non-invasive inelastic light scattering technique is an extremely useful tool wherever phonons or magnons play an important role. We have previously used Raman spectroscopy to study the oxidation state and cation disorder in HTS thin films,^{39,40} manganites,⁴¹ and the disorder-induced collapse of the electron phonon coupling in MgB₂.⁴²

Microcalorimetry: Our ultra-sensitive microcalorimeter can measure heat capacities of microgram samples in high magnetic fields.^{43, 19} In MgB₂ we have used it to measure the heat capacity jump at T_c in single crystals, and in polycrystalline material to obtain H_{c2} and its anisotropy. More recently we have adapted it to measure the latent heat at magnetic transitions independently.⁴⁴ A key aspect of thermodynamic measurements is that they reflect bulk parameters, unaffected by problems of grain connectivity.

High Frequency Properties: We have used microwave probes to determine the penetration depth (λ) and surface resistance (R_s) as a function of temperature in MgB₂,⁴⁵ and obtained evidence for weak link behaviour from microwave properties in applied magnetic field.⁴⁶ In the BCS framework, the

temperature dependence of λ provides information on the density of pairs and on the electron-phonon coupling, so it is an important tool in the study of new superconductors. Microwave measurements of the $\lambda(T)$ for example can offer complementary insight into gap structure and also into order parameter symmetry.

References

- ¹ F. Magnus et al., Nature Materials, **7**, 295 (2008).
- ² Y. Bugoslavsky, G.K. Perkins, et al. Nature **410** (2001) 563.
- ³ K.A. Yates, L.F. Cohen, ZA Ren et al., Point contact Andreev reflection spectroscopy of NdFeAsO_{0.85} Supercond. Sci Techn. **21**, 092003 (2008).
- ⁴ K. Yates et al., Investigation of superconducting gap structure in TbFeAsO_{0.9F0.1} using Point contact Andreev Reflection” New Journal of Physics, **11**, 025015 (2009).
- ⁵ J. Moore et al., “Evidence for supercurrent connectivity in conglomerate particles in NdFeAsO_{1-delta}”, Supercond. Sci Techn. **21**, 092004 (2008).
- ⁶ M. Johannes, Physics **1**, 28 (2008).
- ⁷ Y. Mizuguchi et al., Appl. Phys. Lett., **93**, 152505 (2008)
- ⁸ S. Medvedev et al., Nat Mat **8** (2009) 630
- ⁹ Fletcher et al, Phys Rev Lett, **102**, 147001, (2009)
- ¹⁰ M.A. McGuire et al, Phys Rev B **78**, 094517 (2008)
- ¹¹ D.J. Singh and M.H. Du Phys Rev Lett **100**, 237003 (2008)
- ¹² A.J. Drew et al, Nature Mater, **8**, 310 (2009)
- ¹³ Y.J. Uemura – ArXiv: 0811.546
- ¹⁴ C. Lester et al., Phys Rev B **79** 144523 (2009)
- ¹⁵ Jun Zhao et al, , Nature Materials **7** 953 (2008)
- ¹⁶ H Luetkens et al., Electronic phase diagram of LaO_{1-x}F_xFeAs, Nature Mater, **8**, 305 (2009)
- ¹⁷ C-H Lee et al, J Phys Sco Jpn, **77**, 083704 (2008)
- ¹⁸ K. Kuroki et al, Phys Rev B, **79**, 224511 (2009)
- ¹⁹ PA. Lee et al., Phys. Rev. B **78**, 144517 (2008)
- ²⁰ I.Mazin et al., Phys. Rev. Lett. **101**, 057003 (2008)
- ²¹ M. Eisterer et al., Sup. Sci. Technol. **22** (2009) 065015.
- ²² Y. Nakajima et al., Phys. Rev. B **80** (2009) 2510.
- ²³ Y. Bugoslavsky et al., Phys Rev B **69** (2004) 132508.
- ²⁴ Y. Bugoslavsky et al., Phys Rev B **71** (2005) 104523.
- ²⁵ Y. Miyoshi et al., Phys. Rev. B **72** (2005) 012502.
- ²⁶ Y. Miyoshi et al., Super Sci and Tech., **18** (2005) 1176.
- ²⁷ Y. Bugoslavsky et al., Phys. Rev. B, **72** (2006) 224506.
- ²⁸ KA Yates et al, Appl. Phys. Lett. **91**, 122501, (2007).
- ²⁹ K.A. Yates, et al, J. Phys., conf ser., **97**, 012213 (2008).
- ³⁰ K.A. Yates et al, “Evidence for nodal superconductivity in Sr₂ScFePO₃”, arxiv : 0908.2902.
- ³¹ MA Angadi et al Physica C **177** (1991) 479; A. D. Caplin et al , Supercond Sci & Tech **5**, S161-S164 (1992)
- ³² G.K.Perkins *et al.*, IEEE Trans on Appl Super. **11**, 3186 (2001).
- ³³ G. K. Perkins et al. Super.Sci.Technol. **15**:1156-1159, (2002).
- ³⁴ G. K. Perkins et al., Super.Sci.Technol. **15**,1156, (2002).
- ³⁵ MA Angadi et al Physica C **177** (1991) 479; A. D. Caplin et al , Supercond Sci & Tech **5**, S161-S164 (1992)
- ³⁶ G.K.Perkins et al., IEEE Trans on Appl Super. **11**, 3186 (2001).
- ³⁷ G. K. Perkins et al. Super.Sci.Technol. **15**:1156-1159, (2002).
- ³⁸ J.Moore et al., “Effect of columnar defects on the pinning properties of NdFeAsO_{0.85} conglomerate particles”, accepted for publication Supercond. Sci Techn 2009.
- ³⁹ G. Gibson et al., IEEE Tran. on Appl. Sup. **7** (1997) 2130.
- ⁴⁰ G.Gibson et al. Physica C, **333** (2000), 139-145.
- ⁴¹ N. Malde et al., Solid State Comm., **105**, (1998) 643-648.
- ⁴² K.A. Yates et al., Phys Rev B **68** (2003) 220512(R)
- ⁴³ A. A. Minakov et al., Rev. Sci. Inst. **76** (2005) 043906.
- ⁴⁴ Y.Miyoshi, et al, Rev. Sci. Inst. **79** 074901 (2008).
- ⁴⁵ A. J. Purnell et al., Supercond. Sci. Technol. **16** (2003) 1.
- ⁴⁶ AA. Zhukov et al., Appl Phys Lett **80** (2002) 2347.